Experimental study of the dispersion of a fire suppression agent through a real size nozzle of an aircraft cargo cabin extinguisher system

Raúl Payri[1], Jaime Gimeno[1], Pedro Martí-Aldaraví[1,*], César Carvallo[1]
[1]CMT-Motores Térmicos, Universitat Politècnica de València, 46022 Valencia, Spain
*Corresponding author: pedmar15@mot.upv.es

Abstract
Most of active fire suppression systems consist on injecting an agent into the volume set on fire. In the case of aircraft cargo cabin, the agent used up to date is Halon 1301. In fact, the current level of safety, according to the FAA, is that provided by a volumetric concentration of 6% Halon 1301 throughout a protected fire zone for a duration of 0.5 seconds. However, Halon 1301 is known to contribute to the depletion of Earth's atmospheric ozone layer, and it is going to be ban in the incoming years. The FAA has already defined an equivalent level of safety in terms of the performance (concentration and spatial distribution) of the alternative agent. In this work, two different alternative agents are tested. An injection system has been assembled in order to control the injection pressure and the injection duration, in other words, the agent injected mass. The discharge volume is a rectangular constant volume constant pressure vessel of approximately $0.85\,\mathrm{m}^3$. This vessel is provided with two consecutive transparent windows of $0.75 \times 0.75\,\mathrm{m}$ in order to ensure optical access to the whole injection and mixing process. Liquid phase distribution of the agent inside the vessel is measured by means of Diffuse Back-light Illumination (DBI) technique. Vapor phase distribution, when present, is measured through the single-pass Schlieren technique. Results show a poor performance in terms of spatial distribution of the two alternative agents. The sprays result in narrow jet with little atomization: small cone angle and fast penetration rate. This occurs mainly due to the different thermodynamic properties of these two fluids compared to Halon 1301. Changes in the injection system nozzles need to be done to improve the fire suppression agent distribution into the volume.

Keywords
Fire suppression agent; spray; penetration; cone angle; spatial distribution

Introduction

Fire suppression systems are a requirement for every assembly and/or construction, also on airplanes [1]. Since Montreal Protocol, signed in 1987 and effective since 1989, the use of some suppressant agents such as CF_3Br (bromotrifluromethane, Halon 1301) or CF_2ClBr (bromochlorodifluoromethane, Halon 1211) has been banned for most applications due to their ozone layer depletion effects [2, 3]. In fact, its manufacture was eliminated starting in 1994 [4]. Therefore, some replacement agents have been investigated since then [5]. Refrigerants, such as hydrochlorofluorocarbons (HCFCs), were soon disregarded because they were ozone depleters themselves [6]. Hydrofluorocarbons (HFCs) appear to have no harmful atmospheric effects even though they are far less effective fire suppressants. Particularly, the best available replacement chemicals were C_2F_5H (HFC-125) for onboard aircraft and C_3F_7H (HFC-227ea) for shipboard use [6]. However, to be cost-effective, the suppressant and storage/delivery system must be light and compact, as well as compatible with the host designs of existing platforms [2]. And these possible substitutes require two to three times the mass and storage volume relative to Halon 1301. This would severely compromise their implementation, given the tight weight and space limitations [6]. And it is the main reason why the use of alternatives to halon in the aircraft, though not recommended, is not forbidden yet [7].
Other two alternative suppressant agents being investigated and showing great potential are water [8, 9] and dodecafluoro-2-methylpentan-3-one (FK-5-1-12 or Novec 1230) [10]. Novec 1230 has already replaced Halon 1211 in many total flooding applications and has potential to replace Halon 1301 in others. These two are the ones selected for the present study. Most of the published research on this area focus on combustion and extinguishment capabilities of the alternative compounds [11, 12, 13]. Nevertheless, it is known that high-momentum sprays are useful for quickly dispersing condensed-phase suppressants to the fire and the surrounding compartment to minimize the thermal insult to its occupants or cargo [8]. In this sense, the present investigation focuses on the analysis of the suppressant distribution into the volume where fire could occur.
Halon 1301, once injected through the fire extinguisher system, rapidly evaporates and distributes in the volume due to its low vapor pressure (of $1.4\,\mathrm{MPa}$ at room temperature [14]) and low boiling point ($215.37\,\mathrm{K}$ at atmospheric pressure [14]). A concentration of only 7% by volume in air extinguishes fires by a combination of cooling and interference with the chemical reaction chain of fuel and oxygen [15]. For Novec 1230, the required concentration for extinguishment is slightly lower for class B and surface class A hazards (4.5% and 4.1%, respectively) [16]. It has a lower vapor pressure (of $0.04\,\mathrm{MPa}$ at room temperature [16]) than Halon 1301 but higher boiling point (of $322.35\,\mathrm{K}$ at atmospheric pressure [16]). To the best of authors' knowledge, there are not published requirements in aeronautical applications for water systems yet in order to fulfill the minimum performance standard for halon replacement [17], but its distribution inside the volume is more difficult due to its even higher boiling point (of $373.15\,\mathrm{K}$ at atmospheric pressure) and lower vapor pressure (of $0.002\,\mathrm{MPa}$ at room temperature).

Differences in liquid and vapor distributions of these two alternative agents (water and Novec 1230) in a controlled injection conditions and atmosphere are analyzed. Diffuse Back-light Illumination (DBI) technique is used for visualizing the liquid phase, and single-pass Schlieren for the vapor. The combination of these two techniques allows better understanding of the injection system and how the condensed-phase is distributed. It may help to propose variations in the extinguisher system, particularly the nozzle, if needed.

Material and methods

Test rig, matrix and fluids

A boarded halon fire extinguisher system may consist of only a bottle and a nozzle or a complex arrangement of pipes and nozzles [15]. Several multi-hole nozzles are typically used in systems designed for cargo cabin. A particular arrangement with three nozzles, each of them made of 12 orifices is the one selected for the analysis. In order to simplify the test rig, a nozzle with a single orifice oriented in the axial direction has been manufactured. The geometric characteristics of the orifice are the same as in the boarded system: diameter of $2\,\mathrm{mm}$, length of $1\,\mathrm{mm}$ (which leads to a length-to-diameter ratio of $L/D = 0.5$), straight (no conicity), and sharp inlet and outlet. A sketch with the main dimensions and a picture of the nozzle are represented in Figure 1. The large diameter (more than 5 times the orifice diameter) of the upstream duct ensures that pressure and velocity variations occur at the orifice.

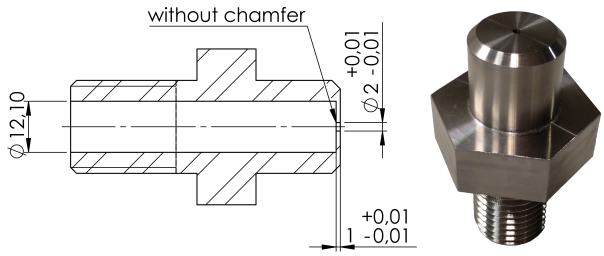

Figure 1. Drawings and picture of the tested nozzle. Units in mm.

Figure 2 sketches the experimental test rig assembly. A pressurized container is used to set the injection pressure (upstream pressure). A 20 MPa pressurized nitrogen bottle is connected to the container and, by means of a manual valve, allows increasing or decreasing the pressure of the container. Before pressurizing, the container is partially filled up with the fire suppression agent (either water or Novec 1230). This container is directly connected to the nozzle with a pipe of 10 mm inner diameter, and a manual ball valve controls the injection. Manometers are used in all deposits and containers to monitor the pressure, as well as thermocouples to monitor the temperature. A piezoelectric pressure sensor is located at the pipe just upstream the nozzle. This pressure signal is utilized to measure the injected mass flow rate and therefore the total injected mass.

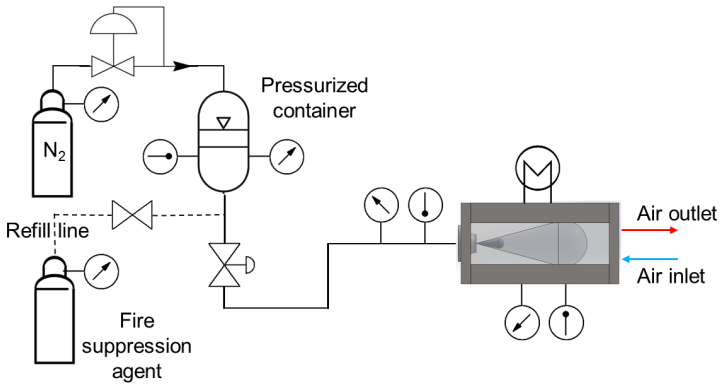

Figure 2. Sketch of the experimental assembly.

A picture of the visualization vessel is shown in Figure 3. It is a rectangular sealed prism with an interior volume of $750 \times 750 \times 1500\,\mathrm{mm}$. This large volume is needed to avoid any interference of the vessel with the spray development. Two transparent windows ($750 \times 1500\,\mathrm{mm}$ in size and $19\,\mathrm{mm}$ thick) are placed on two opposite sides of the prism. Metallic walls ($5\,\mathrm{mm}$ thick) are used for the rest of the faces (the two large plates could be replaced by transparent windows if needed). Although all tests are conducted in quiescent atmosphere, air re-circulation is required. Suppressant vapor phase is heavier than air and thus it may increase the discharge ambient density (up to 7 times if a saturated air and Novec 1230 gas mixture is achieved).
Optical instruments (lenses, cameras, filters...) utilized in the measurements do not allow to record the whole field of view of $750 \times 1500\,\mathrm{mm}$. Therefore, three different positions are selected as fields of view, as represented in Figure 3. The three of them are aligned with the axis of the nozzle, but the exact position and size of each field

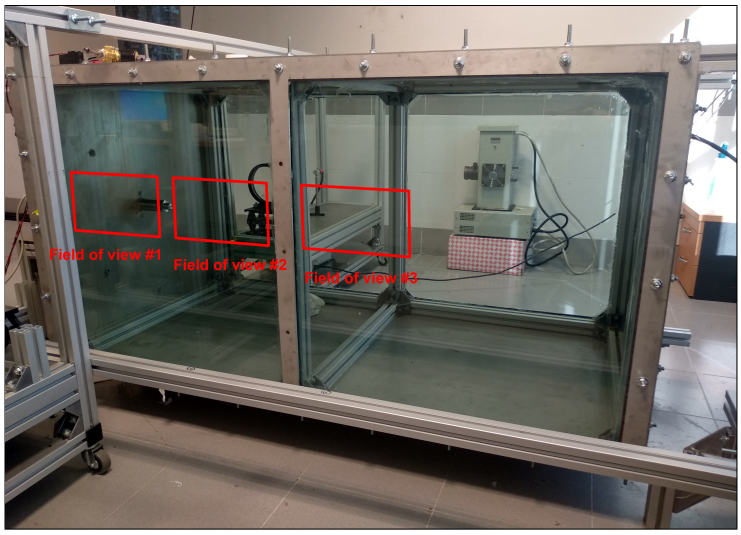

Figure 3. Picture of the visualization vessel.

of view for each experimental technique are given in Table 1, being the reference (position 0 mm) the nozzle outlet section.

Table 1. Position and size of the fields of view.

		Position [mm]	Width [mm]	Height [mm]
DBI	Field of view #1	-18	173	87
	Field of view #2	450		
	Field of view #3	790		
Schlieren	Field of view #1	-11	133	67
	Field of view #2	450		
	Field of view #3	790		

The suppressant to be replaced, Halon 1301, can be stored in a small volume as a liquid at room temperature and pressures greater than 1.61 MPa [4]. The U.S. Army has adopted a standard storage of 5.2 MPa at 293 K [15]. However, to reproduce the injection pressure of real systems, pressure losses in the pipe delivery system need to be taken into account. These depend on the length and bends of the pipes. To cover all possible scenarios, three different values of injection pressure are tested: 1.5 MPa, 2.5 MPa and 5.0 MPa. The ambient conditions are maintained constant at room temperature (298 K) and atmospheric pressure (0.1 MPa). Temperature of the fluid being injected is also kept constant at 298 K.
The two fire suppressant alternative fluids being tested are, as mentioned in the Introduction section, water and Novec 1230. Their main thermo-physical properties [18, 19] are listed and compared to those of Halon 1301 [15] in Table 2. These properties play a major role in spray development, as it will be shown later in this work.

Table 2. Thermo-physical properties of Halon 1301 and the alternative suppressants. All values at 298 K unless otherwise specified. Some uncertainty is present in the value of Novec 1230 surface tension.

Property	Halon 1301	Water	Novec 1230
Chemical formula	CF_3Br	H_2O	$CF_3CF_2C(O)CF(CF_3)_2$
Molecular weight	148.91 g/mol	18.02 g/mol	316.04 g/mol
Boiling point at 0.1 MPa	215.35 K	373.15 K	322.35 K
Freezing point	105.15 K	273.15 K	165.15 K
Vapor pressure	1.47 MPa	0.002 MPa	0.04 MPa
Density	1551 kg/m^3	1000 kg/m^3	1616 kg/m^3
Liquid viscosity	$1.6 \cdot 10^{-4}$kg/(m · s)	$1.03 \cdot 10^{-3}$kg/(m · s)	$3.9 \cdot 10^{-4}$kg/(m · s)
Surface tension	$5.95 \cdot 10^{-3}$N/m	$72.75 \cdot 10^{-3}$N/m	$177 \cdot 10^{-3}$N/m

Diffuse Back-light Illumination (DBI)
DBI consists on the determination of the shape of the spray liquid phase based on the silhouette obtained by the obstruction of a beam of diffuse light with the jet [20]. For the setup utilized in this investigation, the light beam is

produced by a high power continuous light source and goes through a diffuser which homogenizes and smooths the background of the spray image. Most significant details of the setup and hardware are summarized in Table 3. An example of the type of images obtained with this techniques is shown in Figure 4. The gray bar after the second field of view represents the supporting column of the vessel (see Figure 3). It is clearly observed how the liquid phase reaches the end of the third field of view, a distance of about 1 m from the orifice outlet.

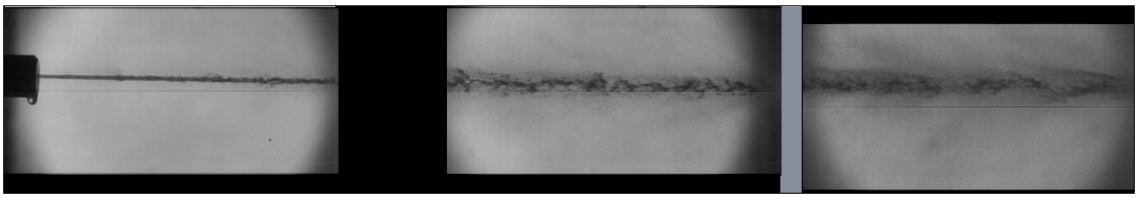

(a) Water.

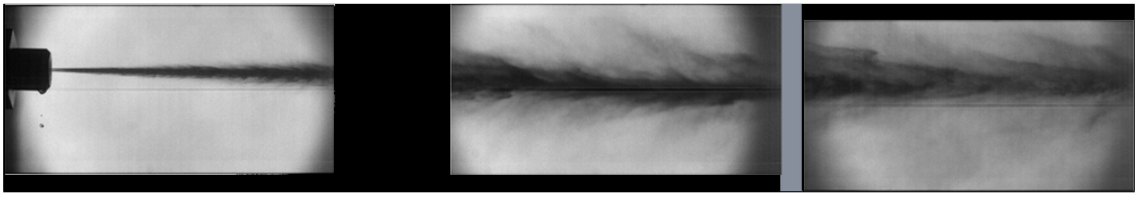

(b) Novec 1230.

Figure 4. Example of the images acquired with the DBI technique. It represents the steady state of suppressant discharge with an injection pressure of 5 MPa.

Single-pass Schlieren

Light rays are deflected when trespassing through a medium with density changes. Schlieren imaging technique makes use of this phenomenon and allows detecting the spray contour by filtering or discarding some of the deflected light [21]. A single-pass setup was used in this investigation. A white-light light was places at the focal length of a collimating lens. After this lens, the now parallel light beams pass through the testing region. The deviated beam is collected by another lens, being a diaphragm located at its focal distance, just before the high-speed camera [20]. Most significant details of the setup and hardware are also summarized in Table 3. As before, an example of the type of images obtained with this techniques is shown in Figure 5. Vapor phase is barely visible to the eye in the first field of view, but for further distances it covers the whole field of visualization. Note that in the end the Schlieren technique was not considered for water because the visualizations showed that the spray did not evaporate under the injection conditions tested.

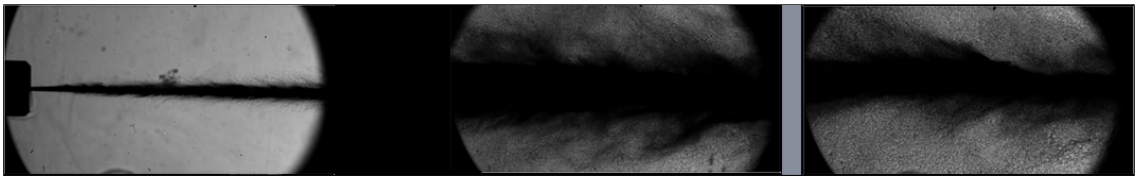

Figure 5. Example of the images acquired with the Schlieren technique. It represents the steady state of Novec 1230 discharge with an injection pressure of 5 MPa.

Table 3. Details of the optical setup for the employed techniques.

	DBI	Schlieren
Camera	Phantom V12	Phantom V12
Sensor type	CMOS	CMOS
Camera lens	55 mm	75 mm
Lenses focal distance	450 mm	450 mm
Diaphragm gap	-	4 mm
Frame rate	11 kfps	11 kfps
Resolution	1024×512	1024×512
Shutter time	20 µs	7 µs
Pixel-mm	3.15	4.225

Image post-processing

It is well known that the image processing is one of the most decisive actions of the analysis of the data. A proper methodology is required to obtain consistent results [22]. In order to obtain the spray contour and so its macroscopic parameters, a previously validated method is employed [20]. It includes: the background correction by subtracting to all images the image just before the start of injection, the spray boundaries detection with a fixed intensity threshold (0.2 for DBI and 0.6 for Schlieren) for differentiating the spray from the background, and the contour analysis. For this last part of the procedure, the spray penetration is calculated as the leading position of the spray contour in the images (for both DBI and Schlieren techniques). The spray angle, for both vapor and liquid phases, is estimated as the angle of the trapezium whose bases are the segments inside the contour that coincide with distances of 12% and 50% of the instantaneous spray penetration.

The sensitivity of these both parameters, penetration and angle, to the fixed threshold value is analyzed in order to verify the robustness of the post-processing technique. The different values used in both techniques are due to the different levels of intensity contrast found in the images (the optical setup is not the same). When the threshold is higher than the selected values, the detected spray contour does not match the one visible in the pictures. Smaller values provide the same results.

The three different fields of view are not recorded simultaneously. In other words, each repetition of each field of view corresponds to a different injection event. The acquired pressure signal on the pipe just upstream the nozzles is used to define the start of injection (SOI) and phase, synchronize, all repetitions and fields of views of the same injection conditions. Up to 5 repetitions of each test point and field of view are performed, acquired and post-processed. The 2 repetitions whose results are furthest from the average are discarded, and the other 3 are used for obtaining the average penetration and angle as well as the standard deviation of those parameters.

Results and discussion

Rate of injection

The discharge of an incompressible non-cavitating fluid through an orifice may be written in the form of Equation 1 [23]. Knowing the discharge coefficient (C_d) of the orifice, the relation between the pressure drop and the mass flow rate is simple. C_d depends mainly on the Reynolds number and the L/D ratio. The Reynolds number ranges from 100000 to 645000 depending on the injection pressure and the fluid, being large in any case. Thus, according to Lichtarowicz et al. [23], $C_d = 0.64$.

$$C_d = \frac{\dot{m}}{A\sqrt{2\rho\Delta p}} \tag{1}$$

Figure 6 shows the time evolution of the mass flow rate for both substances, water and Novec 1230. The average value of all repetitions and all positions for each test condition is plotted together with the standard deviation of the measurements (shaded area). Variations in the measurements are relatively low, which means that the measurements are correct and precise. As expected due to its higher density, the mass flow rate of Novec 1230 is higher. And also, the higher the injection pressure the higher the mass flow. An interesting effect which can be observed is the slow decrease in mass flow rate in the stabilized part of the injection event. This occurs because the pressure in the pressurized container decreases as the injection happens, as the amount of liquid decreases. Larger container would minimize this effect.

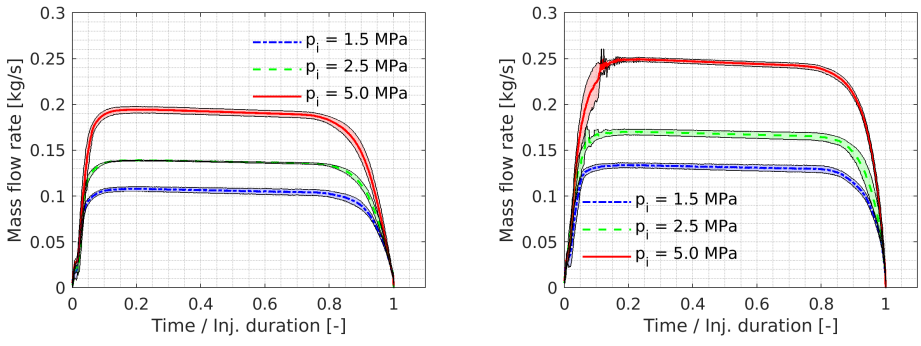

(a) Water. (b) Novec 1230.

Figure 6. Time evolution of the mass flow rate during the suppressant injection event.

The information presented in this section would allow to control the injected quantity by adjusting the injection duration, and so the suppressant agent concentration in the target volume. Nevertheless, actual systems release all the stored agent in case fire is detected.

Spray penetration

Spray penetration curves were obtained after image processing using different thresholds for the detection of the spray contour. This processing routine allows the detection of the maximum distance of the pixels identified as spray

within the detected contour respect to the nozzle exit.
Figure 7 shows the spray penetration curves for each injection pressure and the two fluids used in the experimental campaign. Water has higher spray velocity and so penetrates faster. This happens because the Novec 1230 density is 1.6 time higher than water (which also defines the mass flow rate as shown in Figure 6) and so lower injection velocity. For both fluids, as expected, higher injection pressure leads to an increase of the spray tip penetration [24].

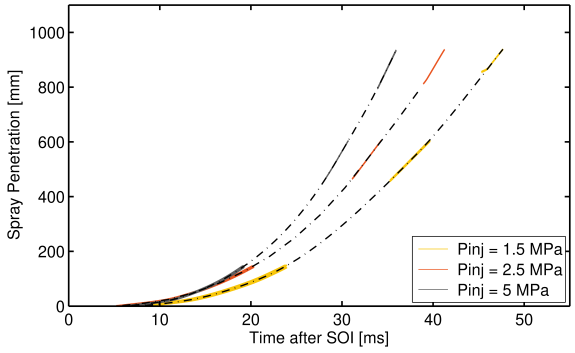

(a) Water.

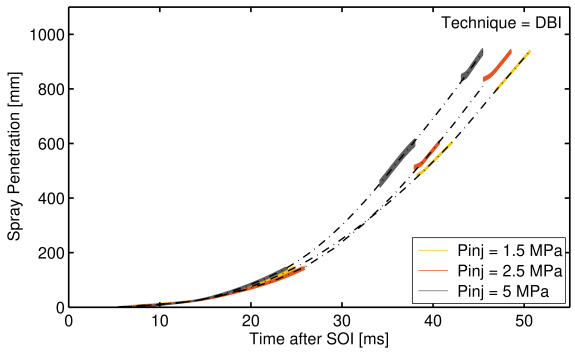

(b) Novec 1230.

Figure 7. Spray penetration results for all the testing conditions.

The shape of the curves changes from a parabolic trend to a straight line due to the fact that in the first moments of the injection process the spray accelerates as it is injected. Afterwards the spray reaches the steady state in which the pressure stabilizes and the spray speed is constant [25].

Spray angle

Figure 8 shows the mean spray angle for different injection pressures. For this result only the field of view #1 was analyzed because as it can be seen in, for example, Figure 5 this field of view is the only one that allows to obtain a reliable spray angle value, the other two are limited by the height of the visualization window. The obtained mean spray angles are narrow for both fluids, between $0.5°$ and $5°$, which results from the poor atomization of the liquid core [26].
There is a small difference between the angles measured by DBI and Schlieren techniques, which means that the liquid evaporation rate is poor. Nonetheless, Figure 5 shows the spray width development from the field of view #1 to the #3 corresponding to a particular test point. It is noticeable that small variations on spray angle lead to a major changes in the spray width far downstream. For this particular case, a spray angle of $5.5°$ produces a spray width of $21.7\,\mathrm{mm}$ and the end of the field of view #1 and of $101\,\mathrm{mm}$ at the end of the number #3. According to this, an increase of $0.5°$ in the spray angle leads to a 9% increment of spray width for the field of view #3. Accurate measurements of this parameter is key for such large sprays.
The effect of the injection pressure on the spray angle is generally small and depends on the particular nozzle geometry and injection conditions [27]. In this particular case there is an increase of about $2°$ when the injection pressure rises from $1.5\,\mathrm{MPa}$ to $5.0\,\mathrm{MPa}$. This could be related to the flow structure inside the orifice. The higher the Reynolds number (higher injection pressure), the higher the turbulent intensity inside the orifice, leading to a wider spray. In fact, analyzing the atomization regime by means of Reynolds, Ohnesorge and Weber numbers, it falls in the Rayleigh regime for both fluids and all injection conditions [28], which is characterized by low atomization, big droplets and long liquid core.

Conclusions

A large volume constant pressure constant volume vessel was designed and assembled in order to test two new alternatives for replacing Halon 1301 in the fire suppression systems on aircraft. Macroscopic spray characteristics such as penetration and angle were obtained by the use of DBI and Schlieren techniques. At the same time, mass

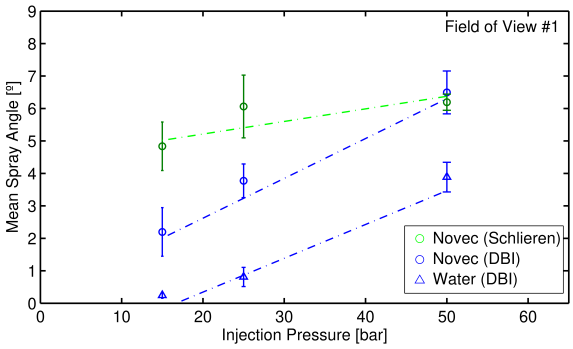

Figure 8. Averaged steady-state spray angle results for all the testing conditions.

flow rate of each injection event was computed from the pressure signal upstream the nozzle.
For these two new agents, water and Novec 1230, most part of the spray was in liquid phase. Additionally, sprays had low atomization with opening angles between 0.5° and 5°. This implies poor agent distribution in the volume. Water injections do not show presence of vapor phase, whilst some vapor Novec 1230 is found with the Schlieren technique around the liquid core jet. Even though, vapor presence is significant only for long distances far from the nozzle exit.
Spray penetration was measured for distances longer than 1 m thanks to the visualization of three different fields of view. Due to its fluid properties, water penetrates into the volume faster than Novec 1230 although its mass flow rate through the orifice is lower. The expected trend when changing the injection pressure is found, the higher the injection pressure the faster the spray penetrates into the ambient.
In spite of the Novec 1230 having an excellent quality as a fire extinguishing agent this will be not enough to reach the maximum possible volume with the actual nozzle geometry used for the experimental campaign. Due to that, geometrical changes to the nozzle are necessary to improve the atomization. In a cargo cabin fire suppression system it is required not only certain agent concentration but also that the fluid reaches the maximum distance and volume possible.

Acknowledgements
This research was performed in the frame of the project “Multi-physics methodology for phase change due to rapidly depressurized two-phase flows” reference 785549 from *Clean Sky Joint Undertaking*. Authors would also like to thank José Enrique Del Rey for his help and participation in the test rig assembly as a lab technician.

Nomenclature

A	area [m^2]
C_d	discharge coefficient [-]
D	orifice diameter [m]
L	orifice length [m]
SOI	start of injection [s]
$\dot{m}$	mass flow rate [kg/s]
p	pressure [Pa]
p_i, p_{inj}	injection pressure [Pa]
t	time [s]
Δp	pressure drop [Pa]
ρ	density [kg/m^3]

References

[1] Hariram, S. S., 2005. “Fire Protection on Airplanes”. *SAE Technical Paper,* ***2005-01-34***, pp. 1–7.
[2] Gann, R. G., 1998. “Next-generation fire suppression technology program”. *Fire Technology,* ***34***(4), pp. 363–371.
[3] Wamsley, P. R., 1998. “Distribution of halon-1211 in the upper troposphere and lower stratosphere and the 1994 total bromine budget”. *Journal of Geophysical Research Atmospheres,* ***103***(1), pp. 1513–1526.
[4] Grosshandler, W., Presser, C., Lowe, D., and Rinkinen, W., 1995. “Assessing Halon Alternatives for Aircraft Engine Nacelle Fire Suppression”. *Journal of Heat Transfer,* ***117***(2), pp. 489–494.
[5] Stoudt, M. R., Fink, J. L., and Ricker, R. E., 1996. “Evaluation of the propensity of replacements for halon 1301 to induce stress-corrosion cracking in alloys used in aircraft fire-suppressant storage and distribution systems”. *Journal of Materials Engineering and Performance,* ***5***(4), pp. 507–515.
[6] Gann, R. G., 2008. “Guidance for advanced fire suppression in aircraft”. *Fire Technology,* ***44***(3), pp. 263–282.

[7] EASA, 2014. Halon: Update of Part-26 to Comply with ICAO Standards.
[8] Yoon, S., Hewson, J., DesJardin, P., Glaze, D., Black, A., and Skaggs, R., 2004. "Numerical modeling and experimental measurements of a high speed solid-cone water spray for use in fire suppression applications". *International Journal of Multiphase Flow,* ***30***(11), pp. 1369–1388.
[9] Li, J., Li, Y. F., Bi, Q., Li, Y., Chow, W. K., Cheng, C. H., To, C. W., and Chow, C. L., 2019. "Performance evaluation on fixed water-based firefighting system in suppressing large fire in urban tunnels". *Tunnelling and Underground Space Technology,* ***84***, pp. 56–69.
[10] Pagliaro, J. L., and Linteris, G. T., 2017. "Hydrocarbon flame inhibition by C6F12O (Novec 1230): Unstretched burning velocity measurements and predictions". *Fire Safety Journal,* ***87***, pp. 10–17.
[11] Grosshandler, W., Hamins, A., Mcgrattan, K., Charagundla, S., and Presser, C., 2000. "Suppression of a non-premixed flame behind a step". *Proceedings of the Combustion Institute,* ***28***(2), pp. 2957–2964.
[12] Gatsonides, J. G., Andrews, G. E., Phylaktou, H. N., and Chattaway, A., 2015. "Fluorinated halon replacement agents in explosion inerting". *Journal of Loss Prevention in the Process Industries,* ***36***, pp. 544–552.
[13] Takahashi, F., Katta, V. R., Linteris, G. T., and Babushok, V. I., 2017. "A computational study of extinguishment and enhancement of propane cup-burner flames by halon and alternative agents". *Fire Safety Journal,* ***91***, pp. 688–694.
[14] Sarkos, C. P., 1975. Characteristics of Halon 1301 dispensing systems for aircraft cabin fire protection. Tech. rep.
[15] Elliott, D. G., Garrison, P. W., Klein, G. A., Moran, K. M., and Zydowicz, M. P., 1984. Flow of nitrogen-pressurized Halon 1301 in fire extinguishing systems. Tech. rep.
[16] ISO-14520-5, 2006. Gaseous fire-extinguishing systems - Physical properties and system design - Part 5: FK-5-1-12 extinguishant.
[17] Reinhardt, J. W., 2012. Minimum Performance Standard for Aircraft Cargo Compartment Halon Replacement Fire Suppression Systems (2012 Update). Tech. rep.
[18] McLinden, M. O., Perkins, R. A., Lemmon, E. W., and Fortin, T. J., 2015. "Thermodynamic Properties of 1,1,1,2,2,4,5,5,5-Nonafluoro-4- (trifluoromethyl)-3-pentanone: Vapor Pressure, (p, ρ, T) Behavior, and Speed of Sound Measurements, and an Equation of State". *Journal of Chemical & Engineering Data,* ***60***, pp. 3646–3659.
[19] NIST, 2003. *NIST Chemistry WebBook, NIST Standard Reference Database Number 69*. National Institute of Standards and Technology.
[20] Gimeno, J., Bracho, G., Martí-Aldaraví, P., and Peraza, J. E., 2016. "Experimental study of the injection conditions influence over n-dodecane and diesel sprays with two ECN single-hole nozzles. Part I: Inert atmosphere". *Energy Conversion and Management,* ***126***, pp. 1146–1156.
[21] Pastor, J. V., Payri, R., Garcia-Oliver, J. M., and Nerva, J.-G., 2012. "Schlieren Measurements of the ECN-Spray A Penetration under Inert and Reacting Conditions". *SAE Technical Paper 2012-01-0456*.
[22] Bardi, M., Payri, R., Malbec, L.-M., Bruneaux, G., Pickett, L. M., Manin, J., Bazyn, T., and Genzale, C. L., 2012. "Engine Combustion Network: Comparison of Spray Development, Vaporization, and Combustion in Different Combustion Vessels". *Atomization and Sprays,* ***22***(10), pp. 807–842.
[23] Lichtarowicz, A. K., Duggins, R. K., and Markland, E., 1965. "Discharge coefficients for incompressible non-cavitating flow through long orifices". *Journal of Mechanical Engineering Science,* ***7***(2), pp. 210–219.
[24] Payri, R., Salvador, F. J., Bracho, G., and Viera, A., 2017. "Differences between single and double-pass schlieren imaging on diesel vapor spray characteristics". *Applied Thermal Engineering,* ***125***, pp. 220–231.
[25] Aleiferis, P. G., and Van Romunde, Z. R., 2013. "An analysis of spray development with iso-octane, n-pentane, gasoline, ethanol and n-butanol from a multi-hole injector under hot fuel conditions". *Fuel,* ***105***, pp. 143–168.
[26] Mayer, W. O. H., and Branam, R., 2004. "Atomization characteristics on the surface of a round liquid jet". *Experiments in Fluids,* ***36***(4), pp. 528–539.
[27] Payri, F., Payri, R., Bardi, M., and Carreres, M., 2014. "Engine combustion network: Influence of the gas properties on the spray penetration and spreading angle". *Experimental Thermal and Fluid Science,* ***53***(September 2015), pp. 236–243.
[28] Reitz, R. D., and Bracco, F. V., 1982. "Mechanism of atomization of a liquid jet". *Physics of Fluids,* ***25***(10), pp. 1730–1742.